A New Unified Compact Model for Quasi-Ballistic Transport: Application to the Analysis of Circuit Performances of a Double-Gate Architecture

S. Martinie[1,2], D. Munteanu[2], G. Le Carval[1], J.L. Autran[2,3]

[1] CEA-LETI MINATEC, 17 rue des Martyrs, 38054 Grenoble, Cedex 9, France
[2] IM2NP-CNRS, UMR CNRS 6242, Bât. IRPHE, 49 rue Joliot Curie, BP 146, 13384 Marseille Cedex 13, France
[3] University Institute of France (IUF), 75000 Paris, France
(e-mail : sebastien.martinie@cea.fr, Phone: +33 4 38 78 18 40, Fax:+33 4 38 78 51 40)

Abstract— **We present here a new unified analytic model for ballistic and quasi-ballistic transport. Starting from the classical approach of Natori, we enhanced it by taking into account degeneracy and adding consistently an original modelling of Short Channel Effect (SCE) and Drain Induced Barrier Lowering (DIBL) by including quantum confinement. Our model has been validated by comparisons with TCAD simulations and results from literature. Finally, we applied our model to simple circuit elements to evaluate potential performance of a Double-Gate architecture in a Verilog-A environment.**

Double-Gate MOSFET, ballistic transport, compact model, Ring Oscillator, quantum effect.

I. INTRODUCTION

Emerging physical phenomena, such as quasi-ballistic and ballistic transport, become to play an essential role in the operation of Double-Gate MOSFET (DGMOS) designed with ultra-short channel lengths. Several pioneering work [1-2] explained the necessity to include quasi-ballistic/ballistic transport into compact model of ultra-scaled devices. This works demonstrated the usefulness of the flux theory for the development of compact models including quasi-ballistic transport. The flux theory is based on the concept of backscattering coefficient which is directly connected to the carrier mean free path. However, considering this advanced transport cannot be dissociated from including a complete description of quantum-mechanical (QM) or short channel effects (SCE/DIBL), which strongly impact the current.

In this work we present an new unified compact model describing the device operation in the quasi-ballistic regime using the backscattering coefficient approach, enhanced by the introduction of the Dynamic Free Path (*dfp*) [3] concept and an analytical description of the Fermi integral [4]. In addition, we implement a new analytical model of the threshold voltage including SCE/DIBL and quantum effects; this threshold voltage model is an analytical description of the numerical development presented in [5]. The paper is organized as follows: section II explains the model equations and the corresponding assumptions; in part III we validate our approach by a detailed comparison with simulation results and experimental data and we highlight the qualitative connection between ballistic transport and the performances of a three-stage ring oscillator based on DGMOS devices.

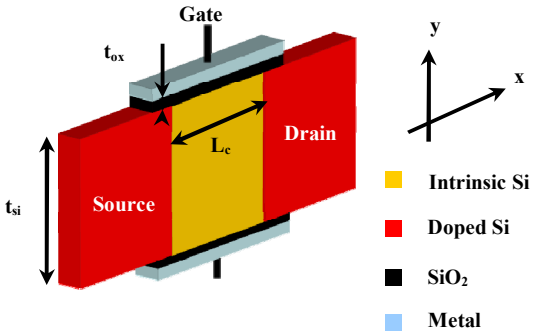

Fig. 1. Schematics of the Double-Gate MOSFET (DGMOS) device used in this work and definition of the main geometrical and electrical.

II. OUR ANALYTICAL MODEL

A. Short channel effects

To find an analytical model for the description of short channel effects, we use the analytical description of the surface potential along the channel developed in [5]:

$$\psi(x) = C_1.e^{m_1.x} + C_2.e^{-m_1.x} - \frac{R}{m_1^2} \qquad (1)$$

where C_1, C_2, m_1 and R are parameters resulting from the Poisson equation solving in the channel [5]. As explained by Suzuki *et al.* [6], the expression threshold voltage shift (ΔV_T) due to SCE/DIBL depends on the value of the minimum potential, defined as [5]:

$$\psi(x_{\min}) = 2.\sqrt{C_1.C_2} - \frac{R}{m_1^2};\ x_{\min} = \frac{1}{2.m_1}.\ln\left(\left|\frac{C_2}{C_1}\right|\right) \qquad (2)$$

ΔV_T is then obtained from equation (2) [5]:

$$2.\sqrt{C_1.C_2} = \Delta V_T \qquad (3)$$

After some algebraic manipulation, we find the analytical expression of ΔV_T which was compared with numerical simulations [7] (Fig. 2) with an excellent agreement.

This work was supported by the Agence Nationale pour la Recherche through project MODERN (ANR-05-NANO-002).

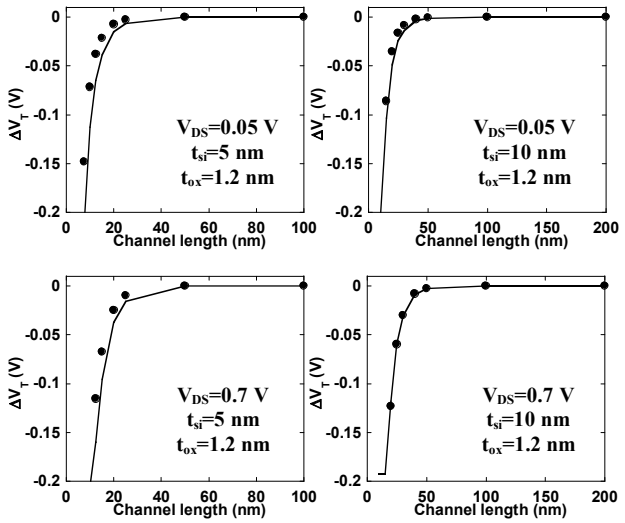

Fig. 2. ΔV_T versus L_c for t_{si}=5 and 10 nm and for V_{DS}=0.05 and 0.7 V. Comparison between our model (solid line) and TCAD simulation (symbols).

In the same way, it is possible to obtain an analytical expression for S-swing parameter using the basic definition:

$$S = \frac{k.T}{q}.\ln(10).\left(\frac{d\psi(x_{\min})}{dV_{GS}}\right)^{-1} \quad (4)$$

B. Quantum-mechanical confinement effects

The expression of the inversion charge Q_i which takes into account quantum-mechanical effects is:

$$Q_i = \frac{q.k.T}{\pi.\hbar^2}\sum_{l,t}\sum_{i} m_{2D}^{t,l}.g_{t,l}.\ln\left(1+e^{-\frac{q}{k.T}.\left(E_{l,t}^{i}+\frac{E_g}{2}-\psi_S\right)}\right) \quad (5)$$

where k is the Boltzmann constant, q is the electron charge, T is the lattice temperature, $\hbar$ is Plank constant, $m_{2D}^{l} = m_t$ $m_{2D}^{t} = \sqrt{m_t.m_l}$, m_t is the transverse mass, m_l is the longitudinal mass, g_l=2 and g_t=4. $E_{l,t}^{i}$ are the energy levels resulting from the quantum confinement of carriers in the Silicon film. As described in [5] this parameter is the sum of two terms: the energy for an infinite rectangular potential and a first-order corrector energy level. We finally obtain:

$$E_{l,t}^{i} = \frac{(\hbar.\pi.i)^2}{2.q.m_{l,t}.t_{si}^2} + \frac{\beta.t_{si}^2}{6}.\left(1+\frac{2}{(\pi.i)^2}\right) \quad (6)$$

$$\beta = \frac{q.N_a}{2.\varepsilon_{si}} + \frac{Q_i}{2.\varepsilon_{si}.t_{si}} \quad (7)$$

where N_a is the channel doping level and ε_{si} is the Silicon permittivity. In the subthreshold conditions the expression of the inversion charge can be simplified as:

$$Q_i = Q^*.e^{-\frac{q.\psi_S}{k.T}} \quad (8.a)$$

$$Q^* = \frac{q.k.T}{\pi.\hbar^2}\sum_{l,t}\sum_{i} m_{2D}^{t,l}.g_{t,l}.e^{-\frac{q}{k.T}.\left(E_{l,t}^{i}+\frac{E_g}{2}\right)} \quad (8.b)$$

We define the threshold voltage, V_T, as the gate voltage for which the inversion charge, Q_i, reaches a constant value $Q_{iT}=C_{ox}.k.T/q$ [5] (C_{ox} is the gate oxide capacitance). Then, the surface potential at threshold is obtained:

$$\psi_S = \frac{k.T}{q}.\ln\left(\frac{Q_{iT}}{Q^*}\right) \quad (9)$$

The threshold voltage is finally calculated as [5]:

$$V_T = V_{th} - \Delta V_T \quad (10.a)$$

$$V_{th} = \frac{\varepsilon_{si}}{\varepsilon_{ox}}.t_{ox}.\beta + \phi_F + \psi_S \quad (10.b)$$

where V_{th} and ΔV_T are respectively the long channel threshold voltage including quantum effects (through the quantum surface potential eq. (9)) and the correction term due to short channel effect (equation (3)).

Figure 3 illustrates the difference between V_{th} in quantum and classical (i.e. without QM) cases. Our model shows also an excellent agreement with the Trivedi and Fossum model [8] (inset of Fig. 3).

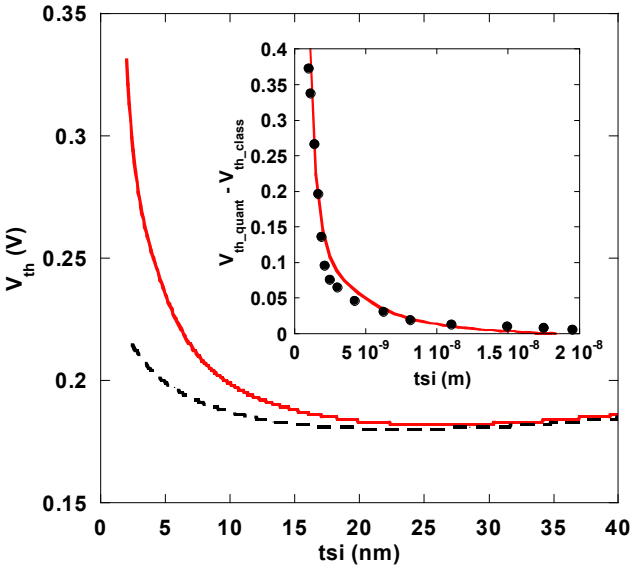

Fig. 3. Threshold voltage versus t_{si}. Quantum (solid line) and classical model (dashed line). [Inset: Difference between quantum and classical approach of threshold voltage (V_{th_quant} - V_{th_class}) vs. t_{si}, comparison between our model (solid line) and the Trivedi and Fossum model [8] (dashed line)].

C. Drain current modeling

Our model of ballistic/quasi-ballistic transport is basically inspired from the Natori/Lundstrom [1-2] approach, extended here to the degenerate case (the analytical model for including the carrier degeneracy is described in [4]):

$$I_D = 2.W.C_{ox}.(V_{GS}-V_T).\frac{F_{1/2}(\eta_F)}{\ln\left(1+e^{\eta_F}\right)}.v_{th}.BR.\frac{1-\dfrac{F_{1/2}\left(\eta_F-\frac{q.V_{DS}}{k.T}\right)}{F_{1/2}(\eta_F)}}{1+BR.\dfrac{\ln\left(1+e^{\eta_F-\frac{q.V_{DS}}{k.T}}\right)}{\ln\left(1+e^{\eta_F}\right)}} \quad (11)$$

where W is the gate width, V_{GS} is the gate voltage, V_{DS} is the drain voltage, $F_{1/2}$ is ½ Fermi integral, η_F is the normalized Fermi level and BR is the ballistic rate [2]:

$$BR = \frac{\lambda}{\lambda + 2.L_{kT}};\ L_{kT} = L_c.\frac{k.T}{q.V_{DS}} \qquad (12)$$

V_T in equation (11) is given by (10.a) and (10.b), and includes QM and SCE/DIBL effects. The above-threshold regime is linked to the subthreshold regime using an interpolation function based on the subthreshold S-swing parameter (equation (4)). This assures the perfect continuity of our model between on-state current (I_{on}) and off-state current.

Finally, we define a "dynamical mean free path" (*dfp*) [3] to include the scattering process with impurities (τ_{imp}), phonon interactions (τ_{ph}) and surface roughness (τ_{sr}). τ_{imp} and τ_{ph} are calculated as in [3] and τ_{sr} is a function used to match the mobility variation versus the inversion charge, following the data of reference [9]. The fitting procedure is illustrated in Figure 4. Then, *dfp* replaces λ to describe the quasi-ballistic transport:

$$dfp = v_{bal}.\tau_{tot};\begin{cases}\tau_{tot}^{-1} = \tau_{imp}^{-1} + \tau_{ph}^{-1} + \tau_{sr}^{-1} \\ v_{bal} = \sqrt{\dfrac{2.\varepsilon_{bal}}{m^*}} \\ \varepsilon_{bal} = \dfrac{3}{2}.k.T + q.V_{DS}\end{cases} \qquad (12)$$

where m^* is the mass in direction of transport, v_{bal} the ballistic velocity, τ_{tot} the total scattering rate and ε_{bal} the carrier energy.

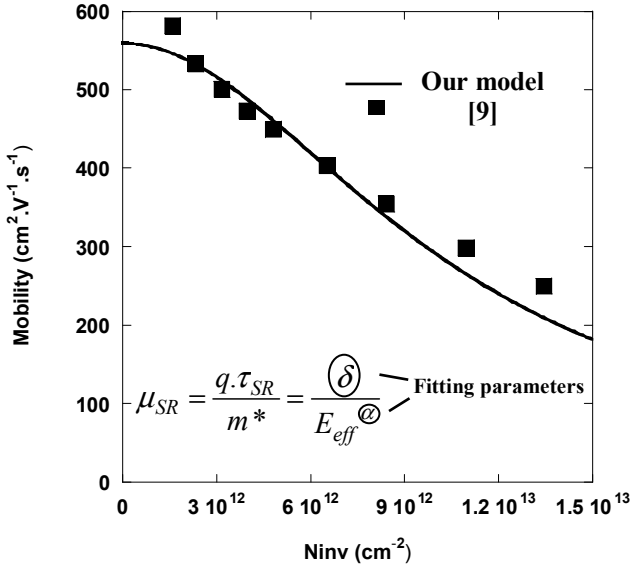

Fig. 4. Mobility versus inversion charge and calculation of τ_{sr}. Comparison between our model (solid line) and data in reference [9] (symbols).

III. SIMULATIONS RESULTS

A. Validation

After implementation in Verilog-A environment, the model has been used to simulate the n-channel DGMOS structure schematically presented in figure 1. To validate our work, we have compared our model with the data of the reference [10]. Figures 5 and 6 represent respectively the drain current versus the gate voltage and the drain voltage for t_{si}=t_{ox}=1.5 nm in ballistic and quasi-ballistic (for the corresponding carrier mean free path of 4.7 nm [10]) case. As expected, our model match very well with data of reference [10] and we have a perfect continuity between the above and the subthreshold regime. Note that the model presented in [10] was also validated by NEGF simulation data in the ballistic case.

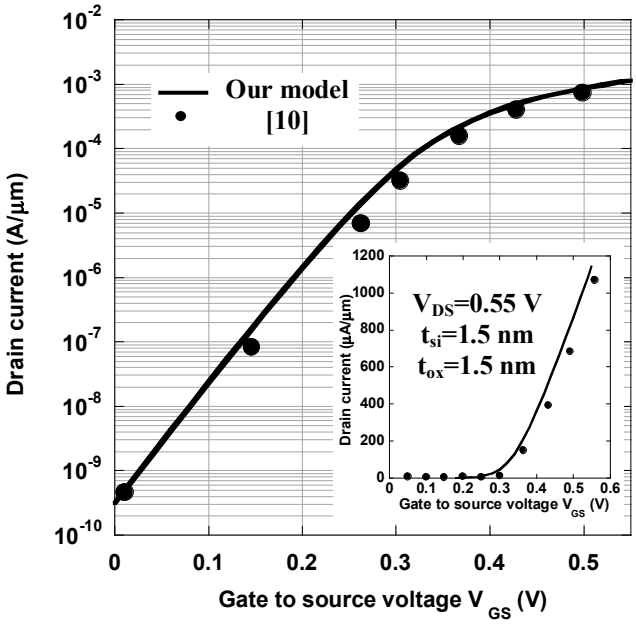

Fig. 5. Drain current versus V_{GS} for t_{si}=t_{ox}=1.5 nm in the ballistic case. Comparison between our model (solid line) and data in reference [10] (symbols). [The inset presents the same simulation in linear scale].

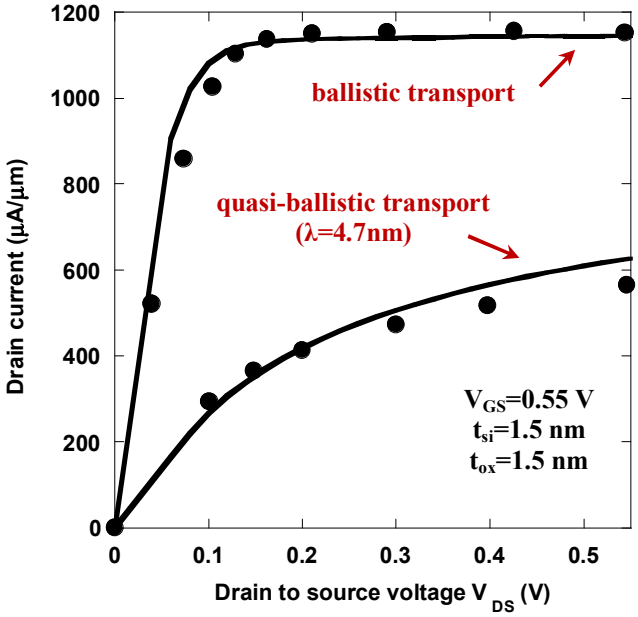

Fig. 6. Drain current versus V_{DS} for t_{si}=t_{ox}=1.5nm in the ballistic and quasi-ballistic case. Comparison between our model (solid line) and data in reference [10] (symbols).

B. Ring oscillator simulation

To clearly highlight the relation between the ballistic/quasi-ballistic transport and the circuit performances, we simulated three-stage ring oscillators. Figure 7 shows the strong

influence of ballistic/quasi-ballistic transport on the oscillation frequency and shows the improvement in transient performances when considering a pure ballistic transport (whatever the charge capacitance). However, it is clear that the short channel effects reduce the difference between the ballistic and the quasi ballistic frequency due to the increase of the propagation time through the CMOS inverter.

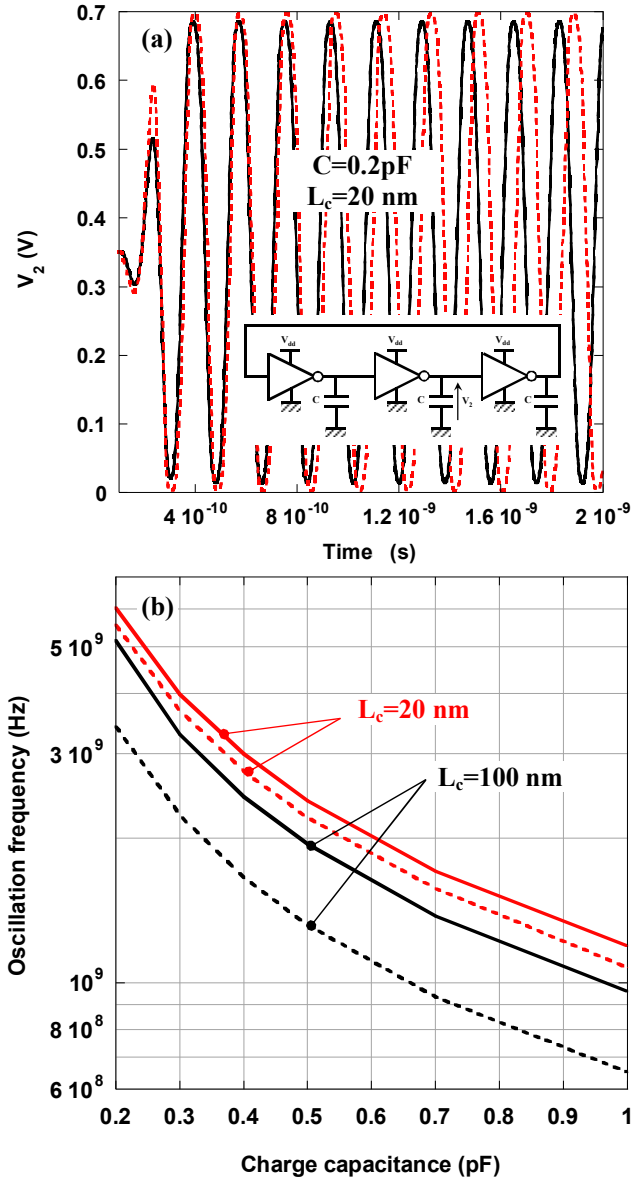

Fig. 7. Output voltage versus time (a) and oscillation frequency versus charge capacitance (b). Ballistic transport (solid line) and quasi-ballistic transport (dashed line).

IV. Conclusion

In this work, a unified compact model for DGMOS taking into account ballistic and quasi-ballistic transport has been proposed and implemented in Verilog-A environment. Short channel effects, quantum-mechanical effects, degenerate statistics and an interpolation function to link the above and the subthreshold voltage have been developed to obtain a unified description of current characteristic. The quasi-ballistic transport has been included by the introduction of new characteristic length: the dynamical mean free path definition was considered to describe scattering processes with impurities, phonons and surface roughness. Finally, the model has been used to simulate a three-stage ring oscillator and illustrate the significant impact of ballistic/quasi-ballistic transport on the switch of CMOS inverter and the oscillation frequency of ring oscillator. Our simulation results demonstrate the strong effect of ballistic/quasi-ballistic transport on oscillation frequency and illustrate the qualitative link between ballistic transport and its impact on circuit performances. However, considering the influence of series resistances will partly modify these conclusions, because the improvements introduced by the quasi-ballistic transport are screened as long as access resistances are important.

Acknowledgment

The authors would like to acknowledge O. Rozeau, M. Reyboz, V. Barral, T. Poiroux, M-A. Jaud, O Bonno and S. Barraud from CEA-LETI MINATEC (Grenoble, France) for helpful discussion.

References

[1] K. Natori, "Ballistic metal-oxide-semiconductor field effect transistor ", *J. Appl. Phys.*, vol. 76, no. 8, pp. 4879-4890, Oct. 1994.

[2] M. Lundstrom and Z. Ren, "Essential physics of carrier transport in nanoscale MOSFETs", *IEEE Trans. Electron Devices*, vol. 49, no. 1, pp. 131-141, Jan. 2002.

[3] E. Fuch, P. Dollfus, S. Barraud, D. Villanueva, F. Salvetti and T. Skotniki, "A new bascattering model giving a description of the quasi-ballistic transport in Nano-MOSFET", IEEE Trans. Electron Devices, vol. 52, no. 10, pp. 2280-2289, Oct. 2005.

[4] S. Selberherr, "Analysis and smulation of semiconductor devices", Springer-Verlag Wien New-York, p. 26 and following, 1984

[5] D. Munteanu, J.L. Autran, S. Harrison, K. Nehari, O. Tintori and T. Skotniki,"Compact model of the quantum short-channel threshold voltage in symmetric Double-Gate MOSFET", Molecular simulation, vol. 31, no 12, pp. 831-837, Oct. 2005.

[6] K. Suzuki, Y. Tosaka and T. Sugii, "Analytical threshold voltage for short channel n+-p+ double-gate SOI MOSFETs", *IEEE Trans. Electron Devices*,vol. 43, no. 5, pp. 732-738, May 1996.

[7] ATLAS Users Manual, SILVACO.

[8] V.P. Trivedi and J.G. Fossum, "Quantum-mechanical effets on the threshold voltage of undoped Double-Gate MOSFETs", *IEEE Trans. Electron Device Lett.*, vol. 26, no 8, pp. 579-582, Aug. 2008.

[9] D. Esseni, M. Mastrapasqua, C. Fiegna , G. K. Celler, L. Selmi and E. Sangiorgi, "Low field of ultra-thin SOI n- and p- MOSFETs: mesurement and implecations on the performance of ultra-short MOSFETs", *IEEE IEDM Tech. Digest*, p. 445-448, 2001.

[10] A. Rahman and M. Lundstrom, "A Compact Scattering Model for the Nanoscale Double-Gate MOSFET", *IEEE Trans. Electron Devices*, vol. 49, no. 3, pp. 481-489, Mars 2002.